Frequency Measurements in a Finite Cylinder Wake at a Subcritical Reynolds Number

M. Budair*
King Fahd University of Petroleum and Minerals, Dhahran-31261, Saudi Arabia
and
A. Ayoub† and K. Karamcheti‡
Florida State University, Tallahassee, Florida 32306

A spectral study of a hot-wire investigation in the near wake of a finite circular cylinder of high-aspect ratio is reported. The measurements included frequency spectra and cross correlations in spanwise and streamwise directions. The study identifies four spanwise regions, in terms of frequency, in the immediate wake of the finite cylinder.

Nomenclature

D = diameter of circular cylinder
d_f = wake width at end of formation region
f = frequency of vortex shedding
l = length of circular cylinder
l_f = formation length
$R_{xy}(\tau)$ = cross-correlation function
U_0 = freestream speed
x = streamwise coordinate (see Fig. 1)
y = crosswise coordinate perpendicular to span of cylinder (see Fig. 1)
z = spanwise coordinate (see Fig. 1)
τ = time

I. Introduction

THE shedding phenomenon over a two-dimensional cylinder had been known for over a century when Strouhal in 1878 introduced the nondimensional frequency fD/U_0, which was shown to stay constant over a wide range of conditions.[1] Later, in 1879, Rayleigh showed through dimensional analysis that the nondimensional frequency, known later as the Strouhal number, is only a function of the Reynolds number.[2] Since then, attempts[3-6] have been made to formulate a universal nondimensional frequency parameter, similar to that of Strouhal, that would hold constant for various bluff cylindrical contours and for a wide range of Reynolds numbers. The unsteady loading on finite cylinders, as well as on infinite cylinders, is important because of its relation to the structural vibrations that pose one of the important engineering problems. The primary source of unsteady loads on cylindrical structures is associated with vortex shedding. In an effort to explain the formation of vortices, Gerrard[7] discussed the mechanism of vortex shedding in which he introduced a formation length l_f within which the vortices form before shedding starts, and a wake width d_f at the end of the formation region. He argued that the frequency of the vortex shedding is based on relating the two lengths.

The vortex structure of the flow past a finite cylinder was addressed for the first time by Taneda[8] who, based on a smoke flow visualization experiment conducted at a low Reynolds number (<100), modeled the vortex structure in the wake of a finite cylinder (see Fig. 1). In his model he suggested that each vortex filament emanating from the tip in one row connects to the two facing vortices in the opposite row, since a vortex filament cannot end in a fluid. At higher Reynolds numbers several attempts were proposed to model the flow near the tip. The experiments conducted by Gould et al.[9] and Etzold and Fiedler[10] suggested a pair of vortices emanating from the tip and springing in the downstream direction. Maull and Young[11] suggested a similar vortex structure over a finite cylinder of noncircular contour configuration. The symmetric pair of vortices suggested in Ref. 10 seems to be in disagreement with the maximum fluctuating lift in the tip reported in the same reference. The shedding frequency measured in the wake of finite circular cylinders of different aspect ratio as reported in Ref. 11 was observed to decrease gradually as the finite end was approached. It was also observed that, for a particular Reynolds number of about 15,000 and an aspect ratio of less than 7, the shedding ceases to occur. Unlike shedding for a two-dimensional cylinder, Fiedler and Wille[12] observed shedding for a finite cylinder of an aspect ratio of 4 at a critical Reynolds number but did not observe shedding at a subcritical Reynolds number. Ayoub and Karamcheti[13] addressed the vortex structure of the flow past a finite cylinder at high subcritical and supercritical Reynolds numbers in which they observed that the shedding phenomenon extends up to a short distance from the tip and the shedding in the tip region corresponds to a lower Reynolds number than the nominal one.

In an attempt to bridge the gap in the range of Reynolds numbers covered in Ref. 13, the present investigation con-

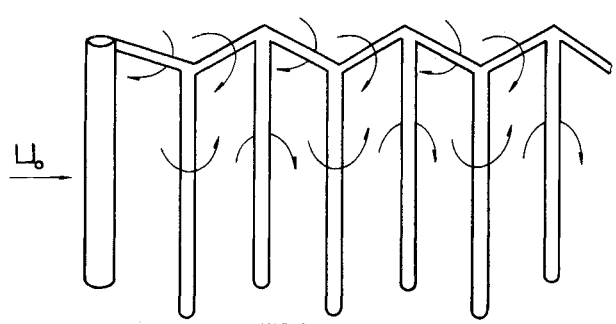

Fig. 1 Taneda's vortex model of the flow past a finite cylinder with Reynolds number less than 100.

Received May 31, 1990; revision received Jan. 10, 1991; accepted for publication Jan. 11, 1991.

*Assistant Professor, Department of Mechanical Engineering, and Director of Aerodynamics Laboratory.
†Member AIAA.
‡Professor, Department of Mechanical Engineering, and Dean of Engineering. Fellow AIAA.

siders the shedding phenomenon on a finite cylinder at a low subcritical Reynolds number. To displace the tip of the cylinder at a relatively large distance from the root, a high aspect ratio model was chosen. The model used has an aspect ratio (l/D) of 37.

II. Apparatus and Experimental Methods

The experimental study was conducted in the 90.2 × 45.7 × 45.7-cm wind tunnel facility of the Department of Aeronautics and Astronautics at Stanford University. The model was a stainless steel bar of diameter 0.635 cm. It was situated at a distance of 53.2 cm from the beginning of the test section and mounted to the vertical wall of the test section at a distance halfway between the lower and upper horizontal surfaces of the test section. The tip of the cylinder was located at about the center of the test section. A sketch of the mounting of the model and the coordinate system is shown in Fig. 2. Two single hot-wire probes were used in this investigation. Their signals from constant temperature anemometers of Disa 55 M10 were linearized by means of Disa 55 D10 linearizers. The sensors were parallel to the span of the cylinder. Their 0.95-cm-diameter supports were connected to two traversing mechanisms outside the upper and lower walls of the test section through grooves parallel to the span of the cylinder (see Fig. 3). The probe connected to the upper traversing mechanism was used as a reference probe, and the other was used as a traversing probe. The two hot-wire sensors could be placed to within 1 mm. A multigroove arrangement in the floor of the test section was used to place the traversing probe at different downstream locations as indicated in Table 1.

The frequency measurement was performed through generating autocorrelation functions and frequency spectra using a correlator of the type Honeywell Model SAI-43A in conjunction with a Fourier transform analyzer of the type Honeywell Model SAI-470. The frequency was thus determined by

Table 1 Streamwise stations at which frequency was surveyed

x/D
0.10
0.97
3.44
6.03
8.53
11.09
13.46

power spectra generated by the analyzer. The spectra were recorded on an x-y recorder for later examination. From preliminary investigation it was determined that the range of frequency did not exceed the 1000-Hz range, and therefore the range in the power spectra was set at 0–1000 Hz with a resolution of 5 Hz.

Vortex shedding was confirmed through cross correlating two signals symmetrically generated from the upper and lower shoulders of the cylinder. A phase shift of 180 deg was the criterion used to confirm the vortex shedding phenomenon. Filtering was necessary in many cases since more than one frequency appeared in the spectra. Since the reference hot wire was limited to a single downstream station, $x/D = 0.10$, the two hot wires could be placed symmetrically to one another with respect to the wake centerplane at only $x/D = 0.10$. At subsequent downstream stations, confirmation of the shedding nature of a frequency component was done as follows: the reference hot wire was placed at the spanwise location where such component appeared, and the traversing hot wire at two symmetrical positions with respect to the wake centerplane. At each position of the traversing hot wire, a cross-correlation function was computed from the signals of the reference and the traversing hot wires. Displaying the two cross-correlation functions led to phase determination.

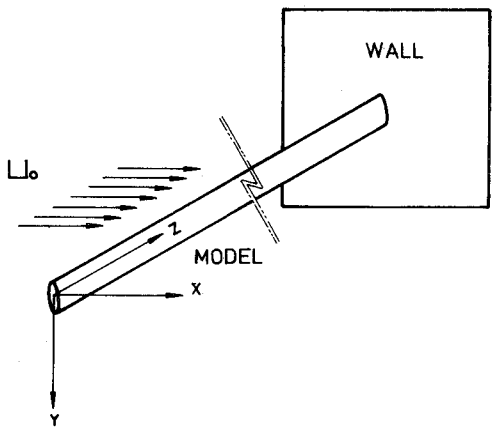

Fig. 2 Finite model with coordinate system.

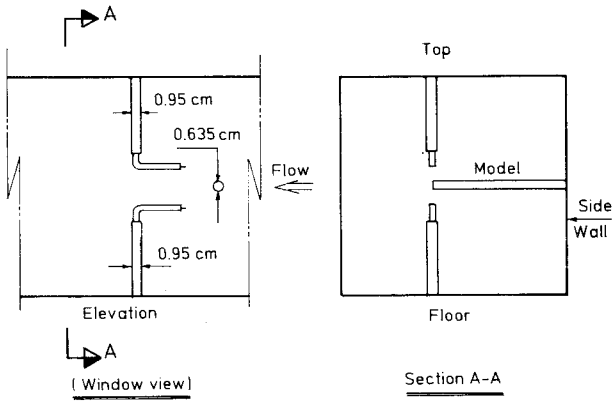

Fig. 3 Sketch of model and hot-wire arrangement.

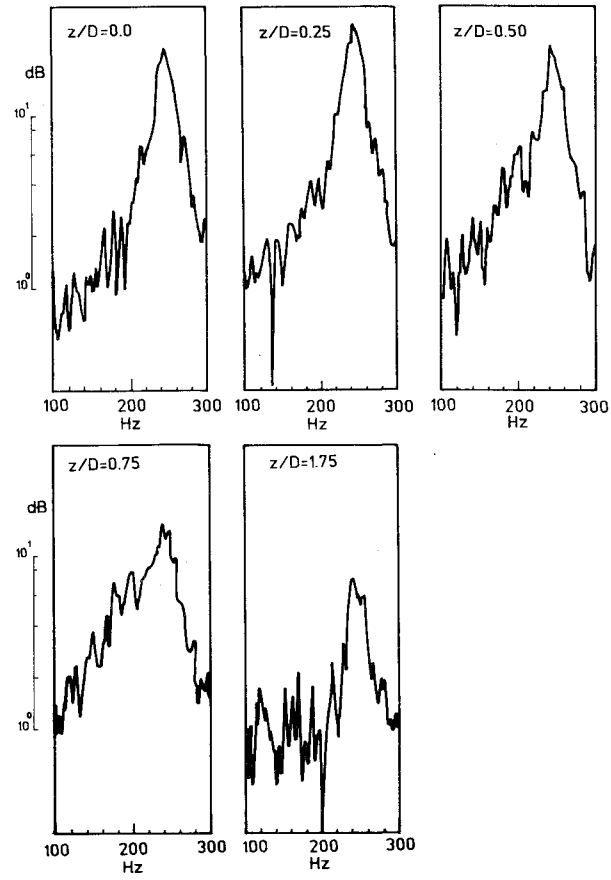

Fig. 4 Frequency spectra of hot-wire signals at $x/D = 0.10$ and $y/D = 0.70$.

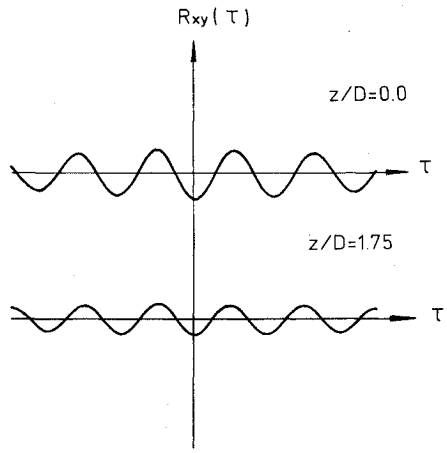

Fig. 5 Cross correlations between two hot-wire signals (filtered between 200 and 300 Hz) at $x/D = 0.10$ with both reference and traversing probes placed at $y/D = \pm 0.70$.

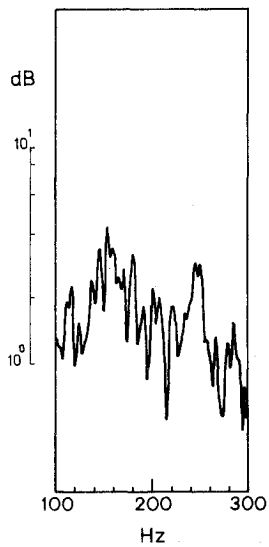

Fig. 6 Frequency spectrum at $x/D = 0.10$, $y/D = 0.70$, and $z/D = 2.25$.

The spanwise movement of the traversing hot wire extended from the tip of the cylinder up to 26 diameters in some downstream stations. The steps at which it was moved were finer toward the tip; they were done in $0.25D$ steps in the first 4.50 diameters from the tip. From $4.50D$ up to $13D$, the hotwire was moved in $0.5D$ steps. Beyond that the steps were not regular because of the two-dimensional region (judging from spectra). The off-wake-center position of the traversing hot wire varied from position to position, but in all cases it was situated toward the edge of the wake.

III. Results and Discussion

A. Finite Model

In this section, results of spanwise frequency survey in the wake of the finite model at different downstream stations (x/D) are reported.

Streamwise Station, $x/D = 0.10$

Figure 4 shows frequency spectra of the velocity fluctuations at $x/D = 0.10$ and $y/D = 0.70$ for different spanwise locations. A distinct spectral peak at 240 Hz is evident at spanwise locations $z/D = 0.0$, 0.25, and 0.50. A check on the nature of this frequency was made by cross correlating the signal from the traversing hot wire with that from the reference hot

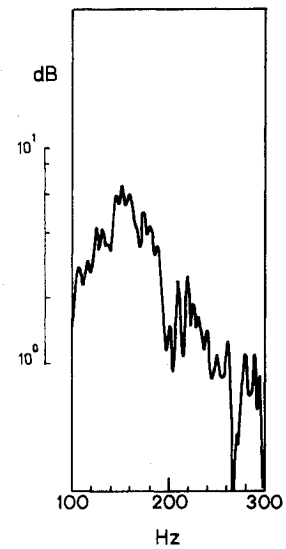

Fig. 7 Frequency spectrum at $x/D = 0.10$, $y/D = 0.70$, and $z/D = 3.0$.

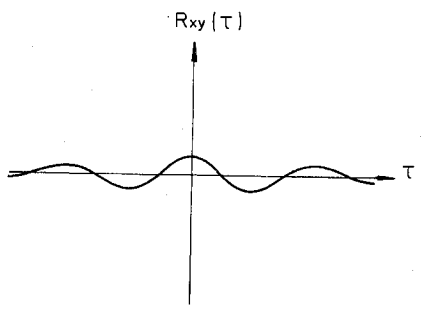

Fig. 8 Cross correlation between signals of traversing and reference hot wires (filtered between 110 and 200 Hz) placed at $x/D = 0.10$, $y/D = \pm 0.70$, and $z/D = 3.0$.

wire with the two hot wires placed at symmetrical positions with respect to the wake centerplane after band-pass filtering between 200 and 300 Hz. The 180-deg phase shift between the two hot-wire signals at $z/D = 0.0$ and 1.75 shown in Fig. 5 is evidence that the 240-Hz component is due to a vortex shedding process. The multipeak spectrum observed at $z/D = 0.75$ is believed to be caused by a slight variation in the shedding frequency. This seems to be supported by the fact that frequency spectra narrowed down over the next diameter without any change in the prominent frequency of 240 Hz, ruling out transitional behavior. Furthermore, the fact that each spectrum was computed from 3200 averages enhanced chances of showing any change in the frequency. At further increase in the spanwise distance beyond $z/D = 1.75$, a lower frequency started to emerge in the spectrum with the already existing 240-Hz component. The new component, characterized by a wide spectrum extending from 150 to 180 Hz, predominated the spectrum gradually in about the next diameter (see Figs. 6 and 7). The nature of this component was checked by cross correlating the reference hot-wire signal with that of the traversing hot wire after placing them in symmetric positions with respect to the wake centerplane and band-pass filtering between 110 and 200 Hz. A zero-deg shift between the signals, shown in Fig. 8, is evidence that this component is not due to a shedding process. As the spanwise distance was further increased away from the tip, another component appeared at $z/D = 3.75$ alongside the nonshedding component manifesting itself by a cluster of peaks around a central frequency of 600 Hz. The central frequency was determined from the time of the first half period of the autocorrelation function. This component predominated the spectrum as the nonshedding component disappeared over the next half di-

ameter. As the distance was increased away from the tip, its central frequency increased and the number of its spectral peaks became less as shown in Fig. 9. A cross-correlation check (Fig. 10) on this component proved that it is due to a shedding process. The word "component" being used to refer to the cluster of frequency peaks is intended to imply that those peaks represent one single component with slight variation in its frequency. Figure 11 shows that this component became single peaked of 700 Hz at $z/D = 13$ and maintained its frequency at farther away spanwise locations in the so-called "two-dimensional" region.

Streamwise Station, $x/D = 0.97$

Similar measurements to the above were performed at this downstream station. The 240-Hz component was discernable from the spectra in the first 2.5 diameters from the tip, as shown, for example, in Fig. 12. A check on this component (Fig. 13) shows two cross correlations between reference and traversing hot-wire signals when the traversing hot wire was placed at two symmetrical positions while the reference hot-wire was at a fixed position. The 180-deg phase shift between the curves for this component is still maintained at this downstream station. The component between 150 and 180 Hz started to be seen at $z/D = 2.75$ with lesser clarity than at the earlier downstream station. The higher frequency component started to appear in the spectra at $z/D = 4.5$ in the form of cluster

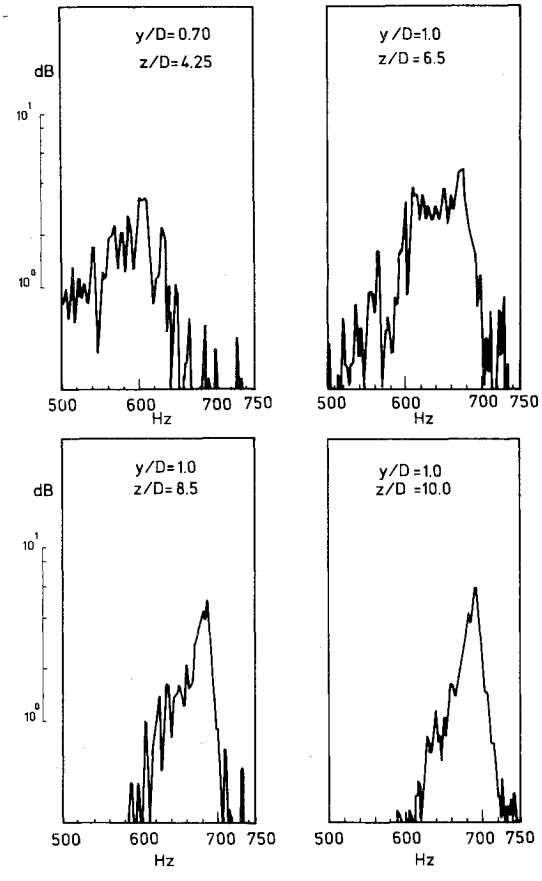

Fig. 9 Frequency spectra of hot-wire signals at $x/D = 0.10$.

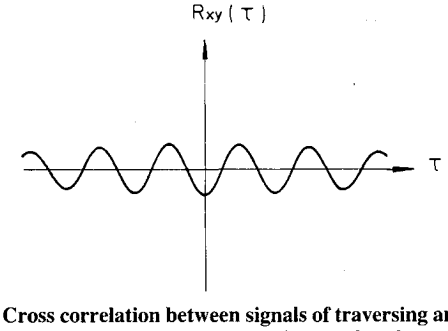

Fig. 10 Cross correlation between signals of traversing and reference hot wire (filtered between 540 and 700 Hz) placed at $x/D = 0.10$, $y/D = \pm 0.70$, and $z/D = 8.5$.

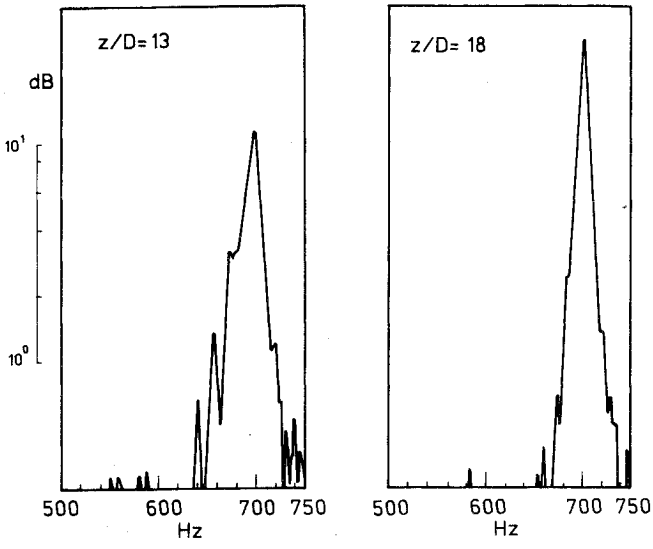

Fig. 11 Frequency spectra of the traversing hot-wire signal placed at $x/D = 0.10$ and $y/D = 1.0$.

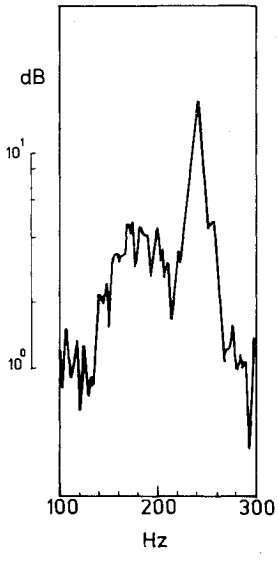

Fig. 12 Frequency spectrum of the traversing hot-wire signal placed at $x/D = 0.97$, $y/D = 0.70$, and $z/D = 0.50$.

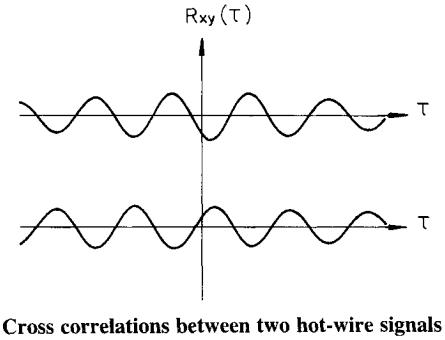

Fig. 13 Cross correlations between two hot-wire signals (filtered between 200 and 300 Hz) with reference probe placed at $x/D = 0.10$, $y/D = -0.79$, and $z/D = 0.0$, and traversing probe at $x/D = 0.97$, $y/D = \pm 0.79$, and $z/D = 2.0$.

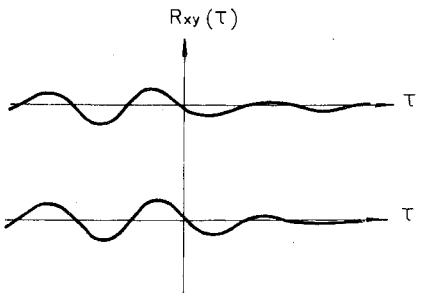

Fig. 14 Cross correlations between two hot-wire signals (filtered between 100 and 200 Hz) with reference probe placed at $x/D = 0.10$, $y/D = -1.0$, and $z/D = 2.25$, and traversing probe at $x/D = 8.53$, $y/D = \pm 3.0$, and $z/D = 1.25$.

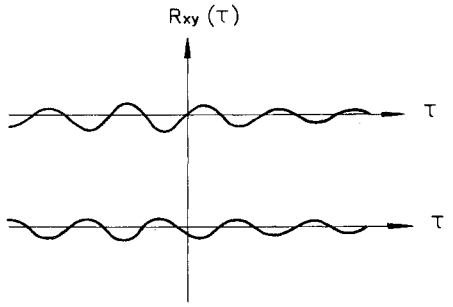

Fig. 15 Cross correlations between two hot-wire signals (filtered between 200 and 300 Hz) with reference probe at $x/D = 0.10$, $y/D = -1.0$, and $z/D = 0.0$, and traversing probe at $x/D = 8.53$, $y/D = \pm 3.0$, and $z/D = 4.0$.

of peaks whose central frequency increased with increasing distance away from the tip. Its uniform single-peaked spectrum of 700 Hz occurred first at $z/D = 14$ and was maintained through $z/D = 26$. It is observed at this stage that in this downstream station the spanwise distribution of frequency follows more or less the same distribution observed in the first downstream station. However, the nonshedding component (150–180 Hz) at this downstream station appeared at a closer position to the tip than at the earlier downstream station. The fact that this component appeared at $x/D = 0.1$ and 0.97 suggests a downstream propagation of this component. Furthermore, the appearance of this component at a closer position to the tip at $x/D = 0.97$ than at $x/D = 0.1$ suggests, as well, a spanwise spread.

Streamwise Station, $x/D = 3.44$

At this downstream station, the 240-Hz component appeared over a distance of 2.5 diameters from the tip. The spectra, however, showed weak appearance of this component as compared to earlier downstream stations. The component (between 150 and 180 Hz) appeared at a very close position to the tip ($z/D = 0.25$) along with the 240-Hz component. The 240-Hz component was not single peaked as had been the case at earlier downstream stations. The characterization check of both components confirmed the shedding nature of the 240-Hz component and the nonshedding nature of the other component (150–180 Hz). The two components at this downstream station and subsequent downstream stations showed poor appearance in the spectra, and therefore the cross-correlation analyses at these downstream locations actually served two purposes: one, as evidence of their existence and, second, as a characterization check of their nature. With cross correlation, it was possible to detect the nonshedding component (150–180 Hz) from the tip location down to a spanwise location of 5.5 diameters. This is a further evidence of the spanwise spread of this component with downstream distance. The high frequency component showed as early as 2 diameters from the tip with a central frequency at about 600 Hz. The uniform single-peaked spectrum of 700 Hz occurred first at $z/D = 13$ and was maintained through $z/D = 25$.

Streamwise Station, $x/D > 3.44$

At further downstream stations the low frequency components, namely, the shedding component (240 Hz) and the nonshedding component (between 150 and 180 Hz), were detected solely by cross-correlation analysis, as shown in Figs. 14 and 15. The high frequency component was always discernable from the spectra. Uniform shedding of this component occurred first at a spanwise distance of 16 diameters away from the tip at downstream stations $x/D = 6.03$, 8.53, and 13.46, whereas at $x/D = 11.09$ uniform shedding occurred first at 15 diameters.

B. Two-Dimensional Model

The vortex shedding frequency was measured at the midspan of the cylindrical model spanning the whole test section. The measurements took place at the respective downstream stations at which the frequency measurements were taken for the finite model. From the spectra the shedding frequency measured was consistently 2% lower than the uniform value observed in the so-called two-dimensional region of the finite cylinder. There is no explanation offered as to why such reduction in frequency was experienced.

IV. Conclusions

A detailed hot-wire investigation of the frequency content in the wake of a finite cylinder of high-aspect ratio is presented. Based on the spectral study, the flow in the immediate wake of the finite cylinder may be divided into four regions: 1) The first is a tip region where shedding occurs at a lower frequency than that in the so-called "two-dimensional" region. It extends to about 2 diameters from the tip. In this range, shedding is more regular as the tip is approached. 2) The second is an intermediate region adjacent to the first region where a nonshedding wideband component exists for about 2 diameters. 3) A third region is characterized by a shedding wideband component whose central frequency increases with the distance away from the tip. The range of this component extends from a distance of about 3 diameters to about 13 diameters away from the tip. The shedding in this range is not regular. 4) A fourth so-called "two-dimensional" region covers the rest of the span except the root region. This region is characterized by regular shedding whose frequency is constant throughout and comparable with that experienced in the wake of the two-dimensional model with a difference of less than 2%.

Both the shedding and nonshedding components in the tip region could be detected further downstream through cross-correlation analysis and to a lesser extent through constructing power spectra. The nonshedding component seems to spread in the spanwise direction as the downstream distance is increased.

Acknowledgments

This research was supported partially by NASA Ames Research Center under Grant NASA NCC 2-75 and King Fahd University of Petroleum and Minerals in Saudi Arabia.

References

[1]McCroskey, W. J., "Some Current Research in Unsteady Fluid Dynamics—The 1976 Freeman Scholar Lecture," *Journal of Fluids Engineering, Transactions of the ASME*, Vol. 99, March 1977, pp. 8–38.

[2]Bishop, R. E. D., and Hassan, A. Y., "The Lift and Drag Forces on a Circular Cylinder in a Flowing Fluid," *Proceedings of the Royal Society of London, Ser. A: Mathematical and Physical Sciences*, Vol. 277, No. 1368, 1964.

[3]Goldburg, A., Washburn, W. K., and Florsheim, B. H., "Strouhal

Numbers for the Hypersonic Wakes of Spheres and Cones," *AIAA Journal*, Vol. 3, No. 7, 1965, pp. 1332–1336.

[4]Goldburg, A., and Florsheim, B. H., "Transition and Strouhal Number for the Incompressible Wake of Various Bodies," *Physics of Fluids*, Vol. 9, Jan. 1966, pp. 45–50.

[5]Roshko, A., "On the Drag and Shedding Frequency of Two-Dimensional Bluff Bodies," NACA TN 3169, July 1954.

[6]Bearman, P. W., "On Vortex Street Wakes," *Journal of Fluid Mechanics*, Vol. 28, June 1967, pp. 625–641.

[7]Gerrard, J. H., "The Mechanics of the Formation Region of Vortices Behind Bluff Bodies," *Journal of Fluid Mechanics*, Vol. 25, June 1966, pp. 401–413.

[8]Taneda, S., "Studies on Wake Vortices," *Reports of Research Institute for Applied Mechanics*, Kyushu Univ., Japan, Vol. 1, No. 4, Dec. 1952, pp. 131–144.

[9]Gould, R. W. F., Raymer, W. G., and Ponsford, P. J., "Wind Tunnel Tests on Chimneys of Circular Section at High Reynolds Numbers," *Proceedings of Symposium on Wind Effects on Buildings and Structures,"* Loughborough Univ. of Technology, Vol. 1, Loughborough, England, UK, 1968.

[10]Etzold, F., and Fiedler, H., "The Near-Wake Structure of a Cantilevered Cylinder in a Cross-Flow," *Zeitschrift fur Flugwissenschaften und Weltraumforschung*, Vol. 24, 1976, p. 77.

[11]Maull, D. F., and Young, R. A., "Vortex Shedding from a Bluff Body in a Shear Flow," *Proceedings of IUTAM/IAHR Symposium on Flow-Induced Structural Vibrations*, Karlsruhe, Germany, 1972.

[12]Fiedler, H. E., and Wille, R., "Some Observations in the Near Wake of Blunt Bodies," *AIAA Journal*, Vol. 8, No. 6, 1970, pp. 1140, 1141.

[13]Ayoub, A., and Karamcheti, K., "Experiment on the Flow Past a Finite Cylinder at High Subcritical and Supercritical Reynolds Numbers," *Journal of Fluid Mechanics*, Vol. 118, May 1982, pp. 1–26.